CIMAC CONGRESS 25
ZURICH, MAY 19 – 23, 2025

2025 | 109

Advanced balance of plant solutions for high-power, high-efficiency and reliable fuel cell systems

Electrification and Fuel Cells Development

Peter Fledersbacher, Woodward

Gregory J. Hampson, Woodward
Ilona Ruoff, Woodward

ABSTRACT

Fuel cells, with their high efficiency and low emissions, are a promising option for many high-power applications such as aircraft, marine, rail and stationary power generation. Fuel cells can play an important role as part of efficient hybrid propulsion systems as well as stand-alone power generation systems, contributing to the decarbonization of so-called hard to abate sectors.

In this context, balance of plant (BoP) components play a critical role in the system efficiency, performance and reliability of fuel cell systems. In our paper, we will address the key challenges related to the PEM BoP for high efficiency and high-power fuel cell systems and provide insights into the development of key components. Key components such as the cathode humidification system, the anode recirculation system, water separation and pressure control both on the cathode and anode side are presented and the design features to address critical functional issues are detailed.

In particular, the air humidification at the cathode side is highlighted since this plays a crucial role in avoiding stack performance degradation and lifetime reductions. To increase power density, PEM FCs are turbocharged with pressure ratio up to 3, resulting in compressor out conditions that are too hot and dry for the FC cathode inlet requirements. Thus, the cathode air needs dynamic conditioning – cooling and humidification - to achieve minimum cathode relative humidity and avoid water droplet condensation and fallout. To achieve these goals, the system must control excess air flow rate, water addition and cathode air heating/cooling. Traditional cathode air humidification using cross-flow membranes has significant short comings (pressure drops, limited inlet temperatures, size and weight) making it less than ideal for highly boosted systems.

In this report, we employ system level analysis and simulation to investigate (or compare) alternatives using first principles 0D FC_RFD tool and 1D GTsuite dynamic system analysis tools. The paper will explore alternative humidification and temperature control systems designed for high boosted PEM FC's which minimizes component number, size and weight, pressure drops, and e-Turbo electrical power consumption and thus overall efficiency.

1 INTRODUCTION

Woodward is a well-known manufacturer of engine components and injection systems used in various sectors like marine, power generation and industrial. The company has recently expanded its product portfolio to include components for hydrogen fuel cell systems. This move is not surprising, given the increasing demand for fuel cell technology as a clean energy solution and the need for well-engineered Balance-of-Plant (BoP) components to ensure efficient and reliable operation, especially for high scaled industrial systems.

Figure 1 schematically shows the complete Balance-of-Plant setup around the fuel cell. The BoP components have a relevant impact on the efficiency and the lifetime of the fuel cell system.

Woodward has developed a new series of BoP components that are specifically designed to enhance the performance of hydrogen fuel cell systems with power outputs exceeding 300kW. These components play a crucial role in the fuel cell system and aid in the expansion of fuel cell systems in various applications.

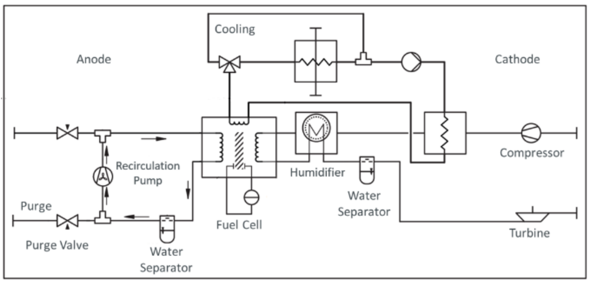

Figure 1. Schematic PEM fuel cell system

1.1 Electrochemical Fundamentals

The Proton Exchange Membrane (PEM) Fuel Cell consists of a catalyzed anode which converts the fuel H_2 into free electrons (e^-) and positive anions (H^+). The PEM membrane, as the name implies, enables the positively charged H^+ ions to diffuse and conduct through the membrane, but is not conductive to the negatively charged electrons (e^-). As a consequence, the electrons build up on the anode side, creating a voltage potential. On the cathode side, a similarly catalyzed surface accepts oxygen (O_2) and the H^+ which has migrated through the PEM membrane to the cathode surface. If a circuit is created to allow electrons to flow from the high electronegatively charged anode to the cathode, the three-component reaction will recombine according to

$$O + 2\,H^+ + 2\,e^- \Rightarrow H_2O \qquad (1)$$

The electrical power generated by the fuel cell results from the current that is allowed to flow through the circuit times the voltage generated by the anode according to P = i V [W]. The power density, P” [W/sqcm], results from the product of the current density, j [A/sqcm] and the voltage V [V] for a single cell. The maximum thermodynamic voltage potential is 1.23 volts for H2 [1], but when any appreciable current is allowed to flow through the circuit, the voltage falls with current density according to the Butler-Volmer equation to typical values between 0.9 volts and 0.4 volts [1].

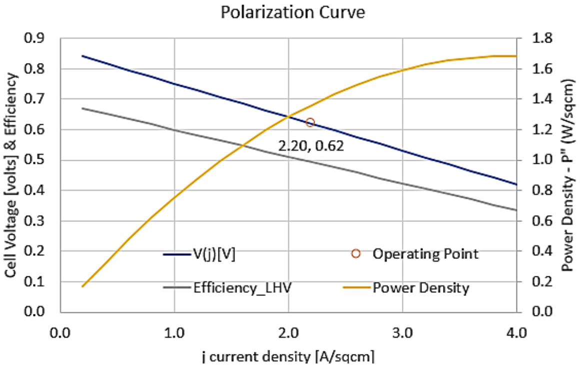

Figure 2. Polarization, Efficiency and Power Density curves for a typical PEM fuel cell

Fuel Cell performance is characterized by the typical polarization curve, an example of which is shown in Figure 2, which shows that the voltage (V) falls with the current density, j (A/sqcm). It also shows the theoretical Lower Heating Value (LHV) efficiency, η = V/1.23 volts. The power density, P”, is shown on the right axis. It shows that as the current is allowed to flow from zero amps to as much as possible, the voltage falls monotonically with the current density. As a consequence, the power density will increase initially as the current increases with a relatively small loss in voltage, but at some point, the voltage drop is greater than the current increase such that the power density reaches a maximum value at a discrete current density, j_{max} (~4.0 A/sqcm in Fig 2). Once this current is reached, the performance drops. As a consequence, it is not beneficial to operate the fuel cell above this max-power current density, since both the efficiency and the power are falling. j_{max} thus represents a maximum useful current density and power density. However, in most cases, the efficiency at this maximum power point is rather low, so the maximum operational current density will be limited well below this to achieve a reasonable efficiency. It is noted that the maximum efficiency is achieved at low current density. In practice, the maximum stack efficiency occurs around 10% of the rated current density. It should be noted that when operating the fuel cell at maximum efficiency, it will also be at the operating point of minimum power density. The impact of this is that to achieve both a high-power output (not density) and high efficiency, a larger active surface area is required, which requires a larger and more expensive fuel cell.

The data shown in Figure 2 may be viewed as the area specific cell performance for a single cell. As there are very few applications which require or can use a voltage of a single cell at, Vcell, which is less than 1 Volt (even less than a standard AA battery) a number of fuel cells are “stacked” and connected in series to increase the voltage, such that if a voltage of approximately 300 volts is required, at least 300 cells must be connected or “stacked”. The FC Stack voltage is thus,

$$V_{stack} = V_{cell}\ x\ N_{cells}\ [\mathrm{V}] \qquad (2)$$

To generate appreciable power from a fuel cell, a relatively large active area is also required, the total current is found by multiplication of the cell active area and the current density according to,

$$i_{cell} = j\ x\ A_{cell}\ [\mathrm{A}] \qquad (3)$$

The stack power is then simply the product of (2) and (3) according to,

$$P_{stack} = i_{cell}\ x\ V_{stack} = (j\ x\ A_{cell})\ x\ (V_{cell}\ x\ N_{cells}) \quad (4)$$

From which we can conclude that if you want to know how a PEM FC stack will perform, all that is required is the polarization curve V = V(j), the active area of a cell, A_{cell}, and the number of cells that are stacked, N_{cells}.

The polarization curve is typically modeled by the Butler-Volmer equation (5), which accounts for *activation losses*, *ohmic losses*, and *concentration losses* [1]. A more detailed version is shown in (6) which shows the voltage falls as the current density, j, increases. This voltage drop is dependent on a number of factors, including the air pressure achieved by the compressor Fig. 3, the humidity of the air in the stack Fig. 4, the temperature, as well as other factors. These figures indicate that shortages of air pressure and/or humidity will negatively impact stack performance. And a note of caution, since air compression is a parasitic power loss for the system, but improves the stack performance, a trade-off analysis would be warranted before finalizing the boost air requirement. The Bulter-Volmer equation is

$$V = E_{therm} - \eta_{act} - \eta_{ohm} - \eta_{conc} \qquad (5)$$

$$V(j) = E_{therm} - (a_A + b_A \ln j) - (a_C + b_C ln\ j) - j\ ASR_{ohm} - c\ ln \frac{j_L}{j_L - j} \quad (6)$$

where, a_A and b_A are Anode constants and a_C and b_C are Cathode constants for the activation loss over voltage, j is the current density, ASR is the “area specific resistance”, and c is the concentration over voltage loss coefficient, j_L is the leakage current. The effects of humidity, temperature, and pressure are included in each of these coefficients.

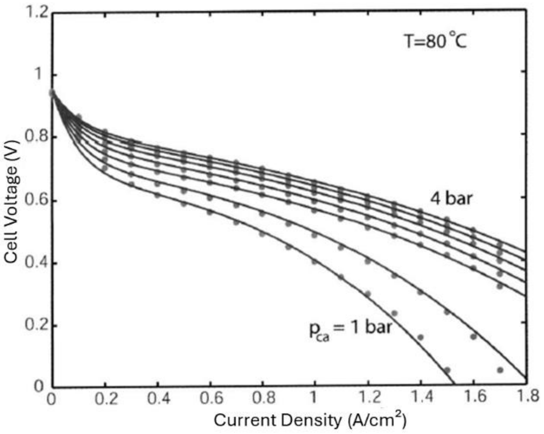

Figure 3. Effect of Boost Air pressure on the polarization curve. [2,4]

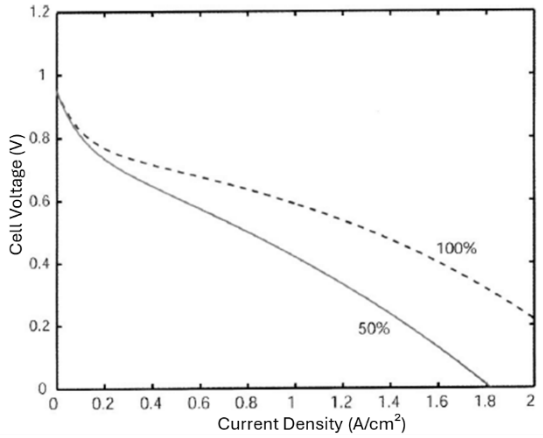

Figure 4. Effect of membrane water content (100°C & 2.5 bar air) on the polarization curve [2,4]

1.2 The importance of excess air flow

To achieve this power output from a FC stack, the hydrogen fuel and air must be supplied and humidified, and the heat and product water removed. For a number of reasons, including humidity, availability, and cooling, the cathode air flow in excess of the stoichiometric O2 consumption rate is required and generally supplied by a blower or compressor. Assuming for example, a stoichiometric excess air ratio of λ_O2 = 2.0, the air flow would be twice the stoichiometric requirement.

Table 1 shows relevant operating parameters for the exemplary case of a 400 kW FC.

Table 1. Air, H2 consumption and Water production rates for 400 kW FC Stack at j = 2.20 A/sqcm, V(j)=0.619 V, Ncells = 350, Acell = 839 sqcm

Key Result	Variable	Value	Units
H2 Consumption	M.H2supply	6.75	[g/s]
Air Consumption	M.airSupply	461.2	[g/s]
H2O Production	M.H20	60.3	[g/s]

Due to the fact that the oxygen in air is only 21% by volume, and since the O2 partial pressure is what drives the O2 diffusion in the cathode, an air compressor is required to achieve appreciable oxygen partial pressure and thus power density and efficiency. And as we shall see in a later discussion, the excess air ratio is required to ensure not only an adequate supply of O2, but also as the carrier of the product water out of the cathode.

To achieve boost levels up to 4 bar, centrifugal compressors powered by an electric motor (e-Compressor) are usually used for this purpose. While additional pressure improves FC power density and efficiency as in Figure 3, the power to run the compressor is appreciable. In this example case, assuming an isentropic compressor efficiency of 75%, the mechanical shaft power of 75.6 kW is required, which represents 19% of the stack power resulting in a significant reduction of power from the FC system (400 kW – 76 kW = 324 kW) with a corresponding reduction in net fuel cell system net power and efficiency. Additionally, power and efficiency losses can be expected from the losses associated with the power management system. Thus, it is not uncommon for these parasitic loads to consume 20-30% of the stack power. Unlike an engine, due to the low temperature air leaving the cathode, a turbine in a fuel cell system, while helpful, can only offset some portion of the compressor power if configured in co-axial e-Turbo (compressor, motor, turbine assembly).

2 WOODWARD BALANCE-OF-PLANT SOLUTIONS AS AN ENABLER FOR EFFICIENT FUEL CELL SYSTEMS

Woodward offers BoP components for both the anode side and cathode side of the fuel cell system as well as for the cooling system and the water system.

Figure 5 is showing examples of Woodward components for BoP items like the cathode air control valve, the anode hydrogen control valve and the control system.

Figure 5. Examples Woodward BoP Components

For example, the Woodward controller platform for Fuel Cells shown in Figure 6 consists of 3 integrated modules:

- MAIN general purpose (Analog I/O and Ethernet)
- EID valve driver (20 current controlled outputs)
- AUX HS processor with (24) analog inputs

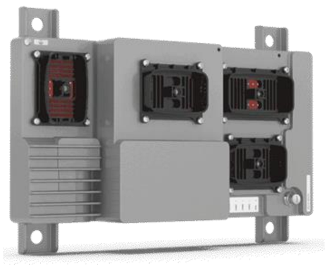

Figure 6. Woodward Controller Platform for Fuel Cell Systems

The control system serves as a crucial component of the fuel cell system, responsible for hydrogen and air processing, thermal and water management. The anode of the fuel cell is supplied with hydrogen. In the anode loop, control valves (Figure 5, image in the middle), shutoff valves and purge valves are provided by Woodward. These hydrogen valves ensure even hydrogen distribution on the anode side and regulate the flow of hydrogen and help to ensure the efficiency and reliability of the fuel cell system. As the anode of a PEM fuel cell is usually operated in an over-stoichiometric condition, the gas mixture at the anode outlet still contains residual hydrogen. For obvious efficiency reasons, it is therefore essential to recirculate this gas mixture back to the anode inlet, where it is mixed with the pure hydrogen fed in.

For this recirculation of residual hydrogen from the anode outlet to the anode inlet, Woodward offers its customers both a passive and active solution. A passive recirculation method utilizes a jet pump, while an active method uses an electrical driven axial recirculation pump. Customized hybrid solutions that combine elements of both methods are possible and they combine the benefits of both methods. Passive recirculation methods use a venturi pump or jet pump to increase the hydrogen flow.

A venturi pump such as shown in Figure 7 utilizes the pressure difference between the main flow and a side flow to draw hydrogen from the side flow into the main flow and needs therefore higher-pressure differences to work efficiently.

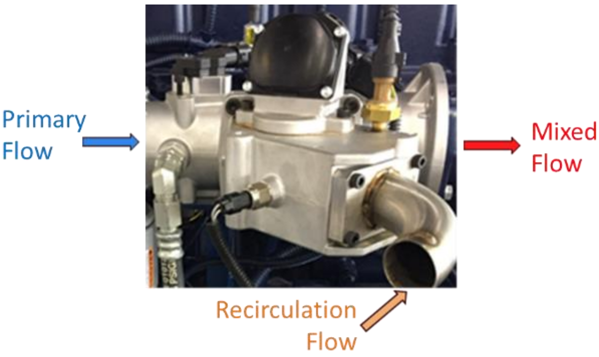

Figure 7. Example passive recirculation device derived from EGR jet pump for ICE application

While the passive recirculation method is the more efficient, its application is limited to high-pressure hydrogen systems and not applicable to LH2 systems. The active recirculation method uses a blower to support the recirculation of the gas mixture composed of hydrogen, nitrogen and water from anode outlet to anode inlet. And it is possible to combine a jet-pump with an active blower.

The development of a blower for the anode recirculation loop presents several challenges, such as:

1. Varying mixture of H2/N2/H2O (liquid + steam)
2. Huge range gas properties (> factor 10 density)
3. Few bearing lubricants compliant with FC
4. Scalability standard automotive solution (side channel blower) is limited (size, weight)

Since at the moment there are no available market options for large fuel cells with unit size > 300kW Woodward has started the development of a lightweight, compact & scalable centrifugal blower (Figure 8).

The aim is to make use of the fundamental advantages of a turbomachine concept in order to achieve a significant increase in efficiency compared to reference systems such as side channel or claw blowers.

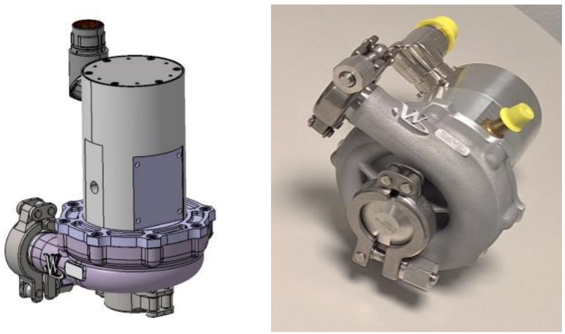

Figure 8. Example active recirculation system, e-driven centrifugal blower

In the anode loop, water can accumulate due to the reaction of hydrogen and oxygen, which produces water vapor as a by-product and the diffusion from the cathode side of the fuel cell. If left unaddressed, this water can accumulate and cause damage to the fuel cell and recirculation pump in the anode loop.

To combat this issue, Woodward has developed proprietary water separators and water drain valves. These components efficiently remove water droplets from the anode recirculating flow, ensuring optimal performance and preventing damage from water accumulation in the fuel cell and cavitation erosion in the blower. More water is typically produced on the cathode side than on the anode side, making it even more important to have effective water management solutions in place. Woodward's water separators and water drain valves help to prevent water accumulation on both the anode and cathode sides of the fuel cell, ensuring optimal performance. Figure 9 shows an example of an integrated solution with the water separator placed in front of the recirculation blower inlet.

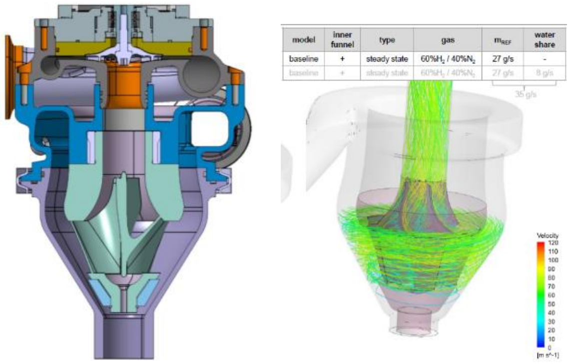

model	inner funnel	type	gas	m_{REF}	water share
baseline	+	steady state	$60\%H_2$ / $40\%N_2$	27 g/s	-
baseline	+	steady state	$60\%H_2$ / $40\%N_2$	27 g/s	8 g/s

Figure 9. Water separator for the anode loop

The water separation is based on imposing a high swirl (Figure 9, right side) on the flow and thus forcing the liquid water components to the outer wall of the separator, from where they can flow downwards.

On the other hand, this swirl at the recirculation blower inlet is not desired, as it would lead to a reduction in the pressure build-up according to Euler's turbomachinery equation. Therefore, after the liquid water has been separated, the remaining gas phase is channelled towards the blower inlet via a flow rectifier element (Figure 10).

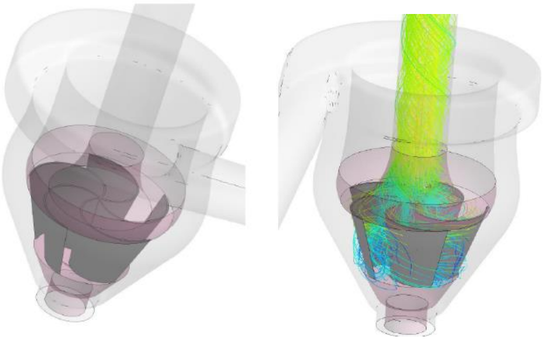

Figure 10. Detail flow rectifier element and flow profile gas phase towards blower inlet

With this flow layout good separation and low pressure losses can be achieved at the same time, which supports the achievement of good overall system efficiencies.

Effective regulation of air is necessary to ensure efficient operation of the fuel cell system. Woodward provides air valves for regulating the cathode side, as well as bypass valves for the humidifier (picture on the left in Figure 5). Woodward’s extensive experience in developing high-performance valves for a range of industries makes them well-suited solutions for fuel cell systems. The air valves used for regulation must be able to handle high flow rates and varying pressure differentials while maintaining precise control over the air supply.

3 WATER MANAGEMENT AND HUMIDITY

3.1 Fundamentals

In the fuel cell system, it is also important to maintain optimized humidity levels. Currently, membrane humidifiers are the standard method for achieving this. However, they have certain drawbacks, particularly when it comes to scaling up the system. Humidification is a critical aspect of fuel cell operation, as it helps to prevent the membrane from drying out and losing its functionality. To ensure the proper functioning of the fuel cell system, it is important to maintain a consistent level of humidity on the cathode side depending on the operational point.

To determine the optimal humidification solution for a highly scaled fuel cell system, Woodward is conducting detailed analyses of the system's operating conditions and performance requirements. This includes 0D, 1D, and 3D-CFD modeling the behavior and performance of alternatives to conventional crossflow membranes such as direct water injection DWI. The CFD analysis is accompanied by extensive testing at the experimental rig at Woodward L'Orange.

Generally, the cathode inlet air conditions for the PEM require 50% to 80% Relative Humidity (RH) at an air temperature between 70°C and 85°C.

From the PEM system description, it is important to point out that the product water will be added to the oxygen depleted cathode airflow which must be removed from the cathode along with the inert N2 in the air. Thus, the cathode air must carry the water required for inlet humidification and have sufficient extra water carrying capacity to absorb the product water and carry it out of the cathode without significant condensation.

These two design requirements create an important design and control problem to flow-down requirements to the excess air flow or stoichiometric air flow, λ_O2, value, which in turn, is dependent on the stack power and water production, as well as the cathode inlet relative humidity. By way of analogy, imagine tanker cars on a train which enter the cathode manifold, but they are already partially full of water to meet the cathode inlet RH requirement, and must carry out the product water with the “available space” in the tanker cars. The design constraints are thus to meet the inlet air humidity and temperature requirements while removing all the product water in vapor form. The free variable is not the carrying capacity of a single tanker car (or kg of air), but the tanker car presentation rate. In other words, the only free variable is the air flow rate, and thus the excess air or stoichiometric ratio, λ_O2. As the load increases, the flow rate (speed of the train) must increase. Consequently, it is not uncommon to target a low excess air ratio early in the design phase to minimize the compressor air parasitic power, but in practice, having to operate at a higher air flow rate to avoid water condensing inside the cathode and stack, and thus a higher compressor power.

To make matters more interesting, if we boost air by a pressure ratio (PR) of 2.7 at full load, assuming a compressor efficiency of 75% the air will be heated above 155°C and even with the ambient air fully saturated at 100% RH (@25°C) the compressor-out RH is still less than 2%. Consequently, the compressed air needs to be both (1) cooled to the stack inlet temperature (<= 85°C) and (2) humidified to at least 50% RH at the cathode inlet temperature.

The system design therefore must include the power level, efficiency, hydrogen consumption, water production, oxygen consumption, air cooling, air humidification and other factors to provide the cathode inlet with the right temperature and relative humidity, and to remove the product water, while minimizing the excess air flow and parasitic power thereof associated. This represents the humidification system design problem we will focus on in this report. For realism, we will use realistic operating parameters for a 400kW stack output as shown in Table 1 and below. In the process, we developed a parametric Requirements Flow-Down model (RFD) which allows us to modify any of the parameters including the power level.

Representative Design Conditions for a 400kW PEM Fuel Cells stack are:

1. <u>Compressor Out</u>
    a. *PR = 2.7*
    b. *TcmpOut = 155.5°C*
    c. *Absolute Humidity, w = 0.0162*
2. <u>Cathode Inlet</u>
    a. *λ_o2 = 2.0*
    b. *M.air = 461 g/s*
    c. *P_cath_In = 2.7 bar*
    d. *T_cath_In = 80°C*
    e. *RH_cathIn = 50% - 80%*
3. <u>Stack</u>
    a. *Water Production, M.H2O = 60.3 g/s*
4. <u>Cathode Outlet</u>
    a. *RH =100%*

For which the design variables are thus:

1. Stoichiometric or excess air flow, **λ_O2**
2. Water addition between the compressor and the cathode inlet, **M.w_inj [g/s]**
3. Air cooling or heating between the compressor and the cathode inlet, **Q_cathIn**

A representative system map with flow rates, power and efficiency is shown in Figure 11.

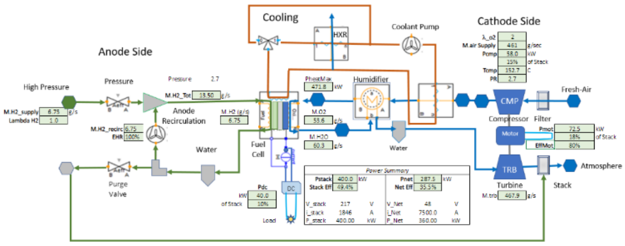

Figure 11. System Diagram from FC_RFD with flow rates, temperatures, power at 400 kW stack power

3.2 Thermodynamics of Air-Water Mixtures relevant to boosted fuel cells

3.2.1 Humidity Requirements PEM fuel cells

To achieve high performance and durability, the PEM membrane must be held at a specific pressure, temperature, and relative humidity, which varies as a function of the power setting.

Humidification Thermodynamics

A quick review of the thermodynamics of air-water and humidity will facilitate the following discussion.

Relative Humidity The equations for humidity are in the Appendix and are summarized here. The key concepts are that in an air-water mixture, the relative humidity (RH) represents the water carrying capacity of the air-water gaseous mixture. At 100% RH, the air cannot carry any more water and is thus saturated. At 0% RH, the air is fully dry, having no moisture. Thus, the RH is scaled from 0% fully dry to 100% fully saturated. Mathematically, this is expressed as the vapor pressure of the water, Pv, relative to the water vapor pressure at the saturated vapor line, Pg: RH= ϕ = Pv/Pg. While the RH is good intuitive measure of the moisture in the air, it is a function of both the mixture pressure and temperature. RH is useful as a “meter” of the “water hunger” of the air, which ultimately drives the vaporization of liquid water, and in the case of fuel cell humidification, the rate of evaporation and mass transfer into the air. Figure 12 provides a useful graph for definitions, showing the water vapor dome with (1) the saturated vapor pressure, Pg at the mixture temperature, Tmix. At the same temperature and the local water vapor pressure, Pv is point (2). If the mixture is cooled at constant pressure, Pv, it will move from point (2) to point (3) where it reaches the dew-point, Tdp = Tsat(Pv), where Tsat(P) and Psat(T) are the saturated vapor functions.

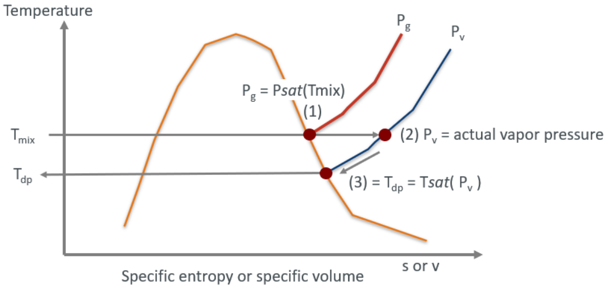

Figure 12. Water Vapor Dome

Dew-Point When an air-water mixture is cooled continuously, the water carrying capacity of the air is reduced as temperature drops; it will eventually reach the point where the water vapor will condense to liquid water droplets. This temperature is called the dew-point, Tdp, which is also the point of 100% RH and fully saturated air. As the temperature continues to fall, more and more water is condensed out to maintain 100% RH in the air. The dew-point temperature is thus the temperature at 100% RH and is often used to define the humidity requirement since it has combines two variables into one and thus is an unambiguous requirement definition. If the water vapor pressure, Pv, is known, then the dew-point is the temperature on the saturation curve at this pressure, i.e. Tdp = Tsat(Pv).

Evaporative Cooling When liquid water is evaporated into air, the latent heat of vaporization of the water is extracted from the surrounding air, thus cooling the air. This is the effect known when air blows over a lake or water mist is used on a hot day to cool air. As illustrated in Figure 13, various quantities of liquid water are added by direct injection into a fixed air stream. As water is vaporized, the air cools. Simultaneously, the dew-point temperature increases as well. As more water is added, the air cools while the dew-point temperature increases, a point is reached where the mixture temperature meets the dew-point temperature, at which point, no more water evaporates, and the air cannot cool any further. Additional water injected does not vaporize, it stays in the droplet form and is carried with the air flow or condense on any surface at or below the dew-point temperature. Figure 13 demonstrates significant cooling potential from direct water injection if the water evaporates, as the temperature falls from 155°C to just above 60°C when fully saturated. Note that 60°C is below the target cathode inlet temperature requirement of 70-85°C.

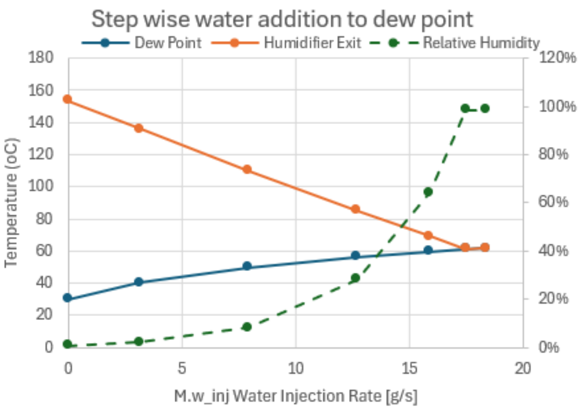

Figure 13. Step by step addition of liquid water in an air stream, initially at 155°C, which is cooled to the dew-point temperature due to evaporative cooling, Relative Humidity (%) is on the right axis

Absolute Humidity The absolute humidity is the ratio of the water mass to the dry air mass, ω = M_w/M_{da}, which is independent of the mixture pressure and temperature, and can be interpreted as the water mass conservation equation normalized on dry air. The utility of the absolute humidity should now be evident; it does not depend upon the pressure or temperature and is immune to discussions of relativeness, dew-point, evaporation or condensation, which makes the mathematics efficient and useful. However, it is only related to mass conservation; it has nothing to say relative to energy conservation or 1st Law Energy Analyses.

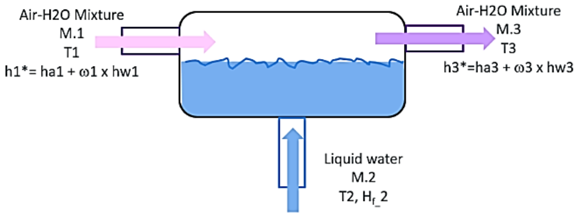

Figure 14. Mass and Energy balance for an Adiabatic Saturator

Energy Analysis Of course we cannot do a thermodynamics analysis with mass conservation, Absolute Humidity, alone; we must also do a 1st Law Energy Analysis. Using the concept of an adiabatic saturator [3], the system is defined by the control volume in Figure 14, where the exit temperature, T3, is determined by the following equation,

$$T_3 = \frac{(Cp_a - \omega_1 Cp_v)\,T_1 + (\omega_3 - \omega_1)\left(h_v^o - h_f^o\right) + (\omega_3 - \omega_1)\,T_2}{(Cp_a - \omega_3 Cp_v)} \tag{7}$$

here, *T* is temperature, *Cp* is the heat capacity at constant pressure, h^o_v, is the standard enthalpy of saturated vapor, h^o_f , is the standard enthalpy of saturated liquid, ω is the absolute humidity, State 1 is at the inlet, State 3 is at the exit, and State 2 is at the liquid water inlet. Eq (7) is the adiabatic saturator energy balance solved for the temperature out of an evaporator, T3. If T3 computed from Eq (7) is found to be below the dew-point temperature, Tdp, will be the lower temperature and no further evaporation will occur; liquid water added beyond this point will remain in liquid form. Thus, the dew-point temperature becomes the limit to Eq (7), according to

$$T3 = \max (T3calc, Tdp), \text{ i.e. } T3 >= Tdp \qquad (8)$$

Psychrometric Chart The key graph to plot points will be the Psychometric chart generated at 2.7 bar, Fig. 15, which shows the absolute humidity, mixture temperature and the relative humidity for air at 2.7 bar. As shown in Fig. 15, the target is indicated with the green box. This defines the required absolute humidity that must be achieved depending on the temperature achieved and RH required. The orange horizontal line is found at the point 80%RH @ 80°C temperature and the green line at the point 50% RH at 70°C as the limits of the “target” box, with a preferred target in the center.

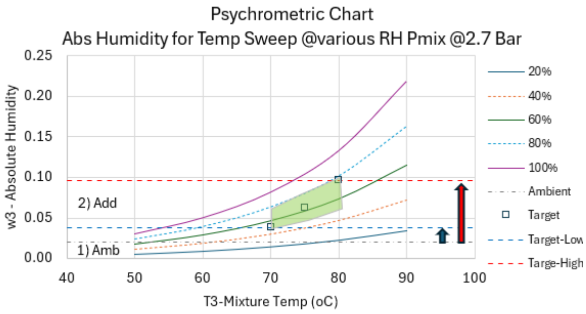

Figure 15. Cathode Inlet RH and T at P = 2.7 bar

3.2.2 Cathode Inlet Humidity Problem

Figure 15 illustrates the cathode humidity problem clearly. Starting at the “Amb” line, the ambient humidity is shown as a dashed horizontal line – in this case 100% RH @25°C with an absolute humidity of 0.021 kgW/kg air. The target cathode inlet humidity on the low side “Target-Low” is 50% RH at 70°C and on the high side “Target-High” is 80% RH at 80°C. From this graph, it appears the solution is simply to hold the temperature constant at the target, 75°C, and simply add the water needed to go from the ambient line to between the Target-Low and Target-High.

However, while apparently straightforward to solve, the problem involves a few challenges: (1) via evaporative cooling, water addition can lower the mixture temperature and (2) the compressor-out point on the ambient water line is very far to the right (2% RH), and that as we add water, the point moves up and to the left along a cooling+humidity sloped line. In which case, the dew-point (100% RH) is reached at a temperature below the target temperature (between 60 and 70°C), which means the added water will drive the operating point to the dew-point and overcool the air before sufficient water is added to meet the target RH at the target temperature. As shown in Fig. 15, at the High-Limit, the maximum absolute humidity is approximately 0.10 gm-water/gm-dry-air and for the Low-Limit, 0.04 gm-water/gm-dry-air. Assuming a given resultant mixture temperature and the absolute humidity ratio of the compressor inlet air, the water addition needed from the compressor inlet to the cathode inlet is determined according to,

$$\omega_{inj} = \omega_3 - \omega_1 \qquad (9)$$

where,

ω_1 = compressor inlet absolute humidity

ω_3 = cathode inlet absolute humidity requirement

ω_{inj} = water to be added before the cathode inlet

It is important to discuss a few points here. First, in many cases, more water is needed to reach the cathode inlet RH at the inlet temperature than that required to reach the dew-point. Which means that while water injection can in theory be used to humidify the compressor-out air towards the cathode inlet requirements, it also cools the air and reduces the potential for vaporization. If water is injected beyond the dew-point, it will not evaporate and will be transported as liquid.

Stack Water Production The final step of the solution is to determine the water production inside the stack, which is added to the cathode air flow. As stated earlier, the nominal goal is for the product water to be carried out of the stack as vapor with the cathode air flow. Keep in mind that the cathode inlet requirements are controlled by the cathode inlet temperature and relative humidity requirements, which determine the absolute humidity ratio target for the water addition, ω_{inj}. Now to ensure that the cathode exit relative humidity is close to 100% and not significantly higher, to avoid water fall out inside the fuel cell stack, the stoichiometric excess air flow defined as,

$$\lambda\_O2 = M.O2\_act / M.O2\_stoich \qquad (10)$$
$$\lambda\_O2 = M.air / M.air\_stoich \qquad (11)$$

the stoichiometric air flow can be determined directly from the water production rate dependent upon the stack electrical power output according,

$$M.air\_stoic = f1(Pstack) \qquad (12)$$

$$M.water\_Prod = f2(Pstack) \quad (13)$$

$$\omega_4 = \omega_3 + \omega_{prod} \quad (14)$$

$$RH4 = f3(T4,\ \omega_4) = 100\% \quad (15)$$

So, the problem definition for the cathode exit (stack out) relative humidity, RH4 defines the excess air flow, λ_O2. Since the model we are using calculates the results of given inputs, the solution cannot be expressed explicitly but will be found for example by executing the solver.

3.3 Modeling and Simulation

3.3.1 Zero-Dimensional Humidification Thermo-dynamics Tools

The equations above have been coded into a 0D-thermodynamic tool. From which the cathode air path stations from ambient to compressor out, water injection, heating/cooling, to cathode-inlet and finally to the cathode out are computed.

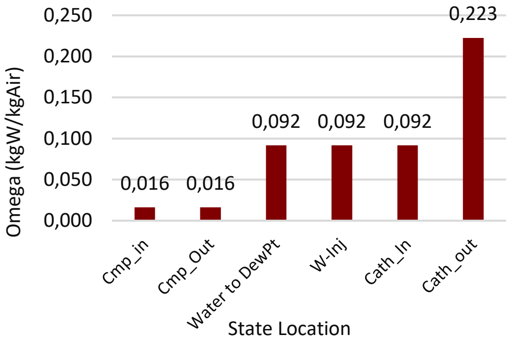

Figure 16a. Absolute Humidity by station

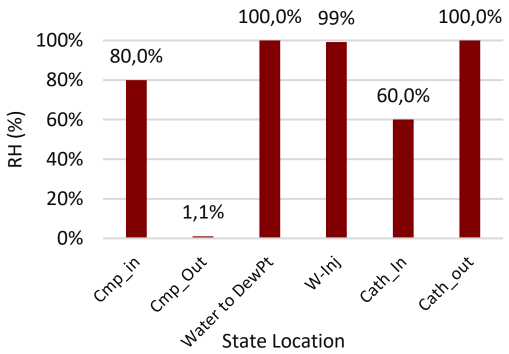

Figure 16b. Relative Humidity by station

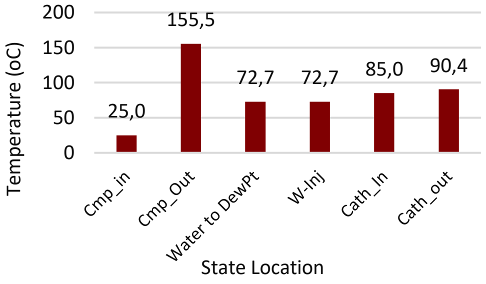

Figure 16c. Temperatures by station

The Figures 16a-c show a direct humidification example with the progression of (a) Absolute Humidity (ω), (b) Relative Humidity (RH), and (c) Temperatures from the compressor inlet through the humidification section, to the cathode-inlet, stack itself, and finally the cathode-exit conditions

3.3.2 One-Dimensional – GTsuite Fuel Cell System Model

The 1D simulations are performed using the higher fidelity fuel cell system model in GT-suite as shown below.

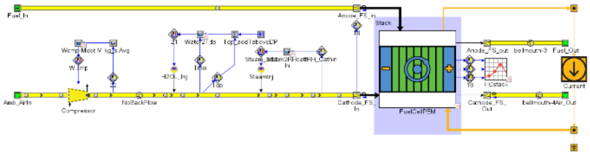

Figure 17. GTsuite FC model with compressor, DWI, and stack

Figure 17 shows the GTsuite Model of the fuel cell system, which includes an air compressor, the PEM submodule, which includes the Polarization Curve shown earlier, the current, voltage and power output. The model also includes liquid and steam injection and a heat exchanger on the cathode inlet pathway. The model was used to confirm the 0D Thermodynamic calculations with full water physics included.

3.3.3 3D Computational Fluid Dynamics (CFD)

3D CFD simulations were performed using the CONVERGE CFD code to explore the sensitivity of evaporation to droplet size. The first study used seeded particles perfectly distributed with the air on the right boundary of the images shown below in Figure 18 for the two cases droplet size 150-micron and 15-micron as well as in Figure 19 for the cases 25-micron and 5-micron. The particle size is imposed along with the air flow rate, temperature and pressure into an air stream within a square cross-sectional duct as an approximation of the LWIU 10.16 cm (4”) diameter pipe 4 meters long. The visual results are shown below. The air flow rate is 420 g/s, the water temperature is 80°C, and water injection rate is according to Table 1.

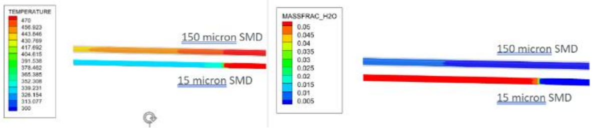

Figure 18. Comparison 150-micron vs. 15-micron droplet size, temperature (red air initial temperature, blue results of evaporative cooling)

and H_2O vapor fraction (blue is all liquid water 0 vapor, red is fully vaporized)

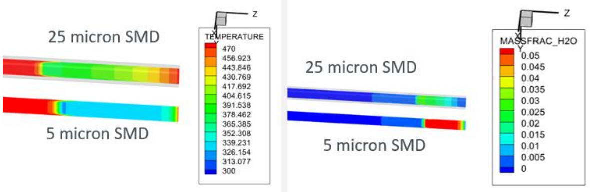

Figure 19. Comparison 25-micron vs. 5-micron droplet size (zoomed in)

The Figures 20, 21 and 22 show the spatial distribution for the various water injection cases. The water vapor fraction and air temperature are shown here for 10 micron seeded water droplets with comparison to the 0D thermodynamic assessment explained previously. In particular, the mixture temperature which includes the evaporative cooling for different absolute humidity per Table 1. Here it is shown that the CFD results converge to the 0D thermodynamic expectations for the same conditions. The results show that (a) 10-micron droplets vaporize and cool the air well within 1 m downstream, (b) 25-micron droplets just achieve full evaporation on the highest absolute humidity case at 4 m, and (c) 50-micron droplets do not reach full evaporation by 4 meters downstream.

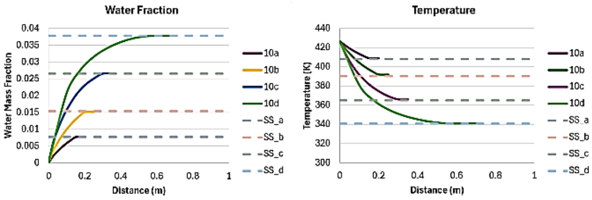

Figure 20. Vaporization & cooling, case 10-micron

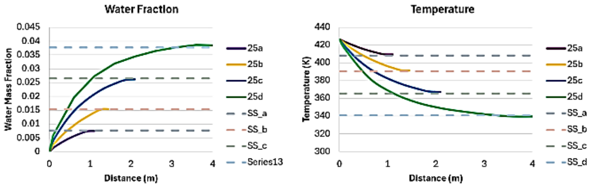

Figure 21. Vaporization & cooling, case 25-micron

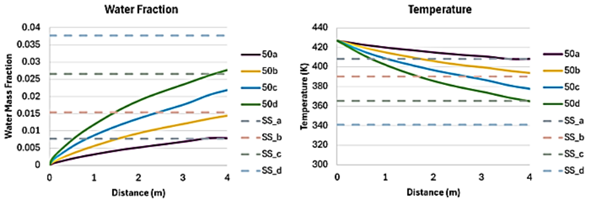

Figure 22. Vaporization & cooling, case 50-micron

From this we can conclude the droplets must be smaller than 25-micron to fully evaporate within 4 meters downstream for this full load condition and the ideal is 10-micron or less.

In contrast to the previous CFD where the droplets were uniformly seeded into the air, now the water droplets are obtained by a hollow-cone injector. Figure 23 shows the CFD resolved droplet radius (upper) and the evaporative temperature (lower) resulting from a spray injection case having an SMD of 25 microns, water Injection rate of 8.75 g/s @ 353 K into air flowing at 420 g/s @ 426 K.

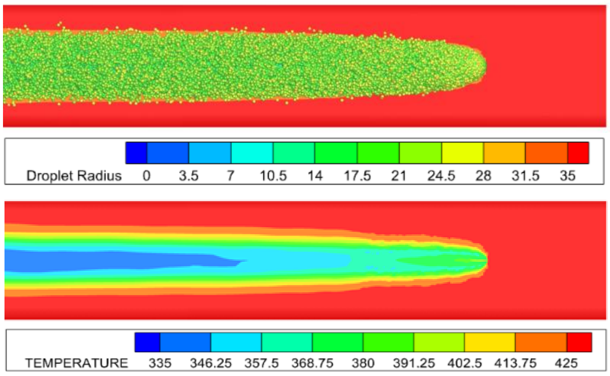

Figure 23. CFD simulation – droplet radius and temperatures due to evaporation

This shows that the droplets that do vaporize, do indeed cool the surrounding air, but that this particular injector example does not well distribute the droplets into the air stream. Clearly, CFD will be necessary to help design the spray characteristics given the flow conditions and that this particular injector is far from optimal as all the droplets are grouped tightly together.

4 EXPERIMENTAL RIG AT WOODWARD L'ORANGE

The cathode BoP component test rig at Woodward L'Orange (Figure 24) is designed to test and validate components for fuel cells up to 500kW unit size.

The air mass flow can be regulated up to 495g/s and temperatures can be controlled up to 150°C. The system operates at a maximum air pressure of 3 bar. Figure 24 shows on the right the inside of the lower test bench container with the climate chamber, in which the ambient temperature can be set from -55°C to 125°C at a maximum humidity of 95%. A Coriolis flow meter next to the climate chamber is utilized to measure the mass flow rate of the cathode air with high precision. The test rig has two air paths – a dry air path and a wet air path. In the wet path the air is humidified by 4 bubble reactors (Figure 24 on the right). When merging both paths in the gas mixer, the air is conditioned to the temperature, pressure, mass flow and the humidity.

One of the additional features of the test rig is the Liquid Water Injection Unit (LWIU). It has a capacity to inject up to 120 liters of water per hour, with adjustable water temperature up to 90°C and water pressure up to 10 bar. The LWIU serves as an additional unit to introduce liquid water into the air stream in the cathode system to test components for example under conditions that can lead to icing (relevant for aircraft applications).

Figure 24. Cathode BoP Component Test Rig

4.1 Experimental investigations on direct humidification

The LWIU can also be used to investigate conceptual approaches like the direct humidification of the cathode described above. To achieve various levels of humidification, water is directly injected into the air stream using a water nozzle. For this purpose, a lance is embedded in the middle of the pipe with a replaceable nozzle (Figure 25). The injected water is intended to evaporate fully to prevent any liquid droplets from reaching the fuel cell, as the presence of droplets can be detrimental to its operation.

In order to investigate the whole evaporation process in detail, the system includes a transparent tube (Figure 25) and is equipped with high-speed cameras and specialized lighting for visual examination. The high-speed camera captures detailed images to determine whether any droplets are still present or if the water has fully evaporated, as ideally required.

To complement the simulation results shown in the section above, tests with different nozzle geometries and operating parameters are performed with this test bench setup. The preselection of the nozzles in order to perform the DWI tests effectively is done on a Phase Doppler Anemometry (PDA) test bench based on the criteria for the droplet sizes shown in Chapter 3.3.3. In this way, the simulation-based investigations into various nozzle configurations can be accompanied experimentally and important findings for the development of DWI systems can be obtained.

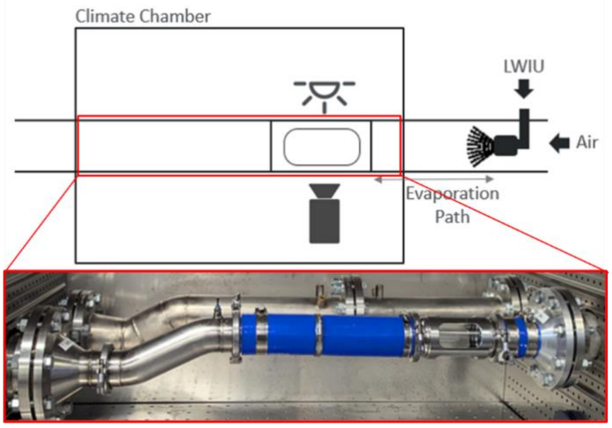

Figure 25. Schematic of the test rig and photo with the transparent pipe in the flow path

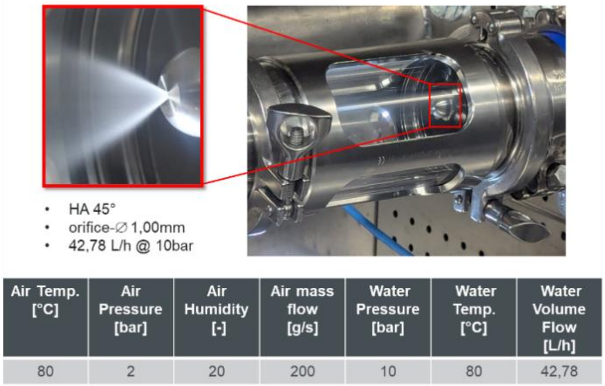

Air Temp. [°C]	Air Pressure [bar]	Air Humidity [-]	Air mass flow [g/s]	Water Pressure [bar]	Water Temp. [°C]	Water Volume Flow [L/h]
80	2	20	200	10	80	42,78

Figure 26. DWI with an extended lance and a BETE nozzle including the test conditions

An example spray tests is shown in Fig. 26 with the initial nozzle configuration and the corresponding operating conditions.

This setup allows the observation of the air-water mixture directly at the water nozzle with an extended lance (Figure 26, right side) or after the evaporation path.

5 DESIGN REQUIREMENTS FLOW DOWN

The humidification problem is now clearly defined: Firstly, the compressor-out temperature is too high and the relative humidity too low for the cathode inlet requirements, thus water needs to be added, *and* the temperature reduced to meet the air cathode air temperature and relative humidity requirement. Secondly, given the absolute water content entering the cathode, the overall flow rate, as expressed by the oxygen excess air lambda (λ), must be set so that the cathode air has sufficient water absorption capacity to remove the stack product water generation rate without significant condensation (RH~100%).

To solve the first problem, the ideal “design space” shown in Fig. 15 but shown again here in Figure 27 below for convenience.

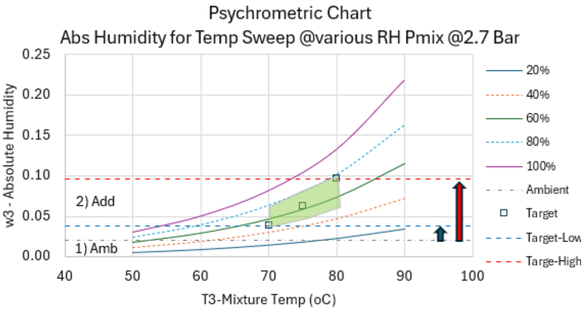

Figure 27. Psychrometric Chart showing the absolute humidity and a window for water addition levels to achieve the cathode in RH.

This is a Psychrometric chart, but not the usual one, this one is developed from the equations explained earlier at the cathode pressure at full load of 2.7 bara. What is shows is the absolute humidity on the Y-axis, the mixture temperature on the X-axis and the relative humidity iso-lines in the graph itself with their designation in the legend. This can be used to map the Humidity-Temperature Trajectory from ambient through the compressor, cathode-in and cathode-out conditions. Most notable is the 100% RH line (purple solid) which limits the operating space to points on or to the right of this line; no point can exist to the above or to the left of this line.

From understanding this point of view, if a state starts to the right as water is added co-current cooling occurs, as the point moves towards this line, the relative humidity will eventually increase to the saturation limit (100% RH) at which the mixture temperature has reached the dew-point temperature and any further water injection will neither increase the RH nor further cool the air-water mixture.

To use the figure, we compute the absolute humidity for the ambient air before the compressor at T_{amb} and RH_{amb}, and then compute the absolute humidity, this generates the lower horizontal line (1) Amb. Compressor heating moves the point along this line from far to the left (25 °C) to far to the right (155 °C off scale), but the line remains constant for constant water content in the air. The two other horizontal lines represent the target absolute humidity for acceptable on the high limit and acceptable on the low limit. These are easy to compute by just identifying the target cathode inlet temperature, i.e. 75 °C and the target RH, i.e. between 50% and 80% iso-RH lines. The green rectangle shows an example target area 50% < RH < 80% and 70 < Temp < 80. The design objective is then to start at the (1) ambient line at the compressor-out temperature and via a combination of water addition and heating, arrive in this target box.

Looking at the cathode air humidification by itself, we propose that since the compressor-out temperature is quite high (155 °C) and above the boiling point of water (100 °C at sea level by lower at altitude) and that ultimately we need to humidify this air (which has a RH of 2% or less at full load), that the evaporative cooling effect of water injection can be used to reduce the cathode air stream temperature – with a double benefit of reducing both the temperature while simultaneously increasing the absolute and relative humidity.

The requirements flow down goes something like this, given (1) amb T and RH => calculate the Ambient Absolute Humidity - the amount of water to add on a dry-air specific and absolute quantity. This generates the Water Injection Requirement (rate and quantity). Next, for this flow rate and to achieve full evaporation to the limit of the dew-point with cooling to the dew-point within the time allowed for the water to travel from the injector to the cathode, the droplet size must be identified (see above, less than 25 micron). Once the maximum droplet size and distribution (SMD) is defined, then the next level flow down is the nozzle design (orifice size and any break-up assistance method such as air-assist). From which the water injection pump or other mode of delivery is defined including the water and air injection pressure requirements.

While this seems straightforward at the outset, we found some challenges. Firstly, our study found that the water addition requirement is greater than the water required to cool the air to the dew-point, which in this case is about 72°C, a temperature below the cathode inlet temperature. Which means more water is required than that to reach the dew-point and more heat is required to fully vaporize all the cathode inlet water requirement to the cathode inlet temperature, in other words, we will reach the dew-point and over-cool the air before we add all the necessary water.

One outcome of the design optimization is a Water-Temperature-Trajectory to achieve (1) the target cathode inlet conditions and (2) to not exceed 100 % RH coming out of the stack. Figure 28 shows the trajectory from the compressor to the cathode inlet and to cathode-stack outlet. In one configuration, the air enters the air compressor, where it is compressed and heated at constant absolute humidity. In the next section, water is added by one or more “direct delivery” methods (e.g. direct spray injection, DWI), where-in the water vaporizes and cools the air via vaporization cooling. At this point, the air is over-cooled and under-humidified. The water addition cools the charge *below* the cathode inlet temperature, and while the local humidity rises to 100% RH as the temperature drops to the dew-point, the absolute humidity is still below the target value for the cathode inlet conditions if the air is heated to the target temperature. To achieve the cathode inlet, both re-heat and additional water are required. One method, to achieve this is to add a heat exchanger and a second water addition stage, which could be traditional membrane humidifier or DWI.

The images below in Fig. 28 are for just one illustrative example. The Water-Temperature-Trajectory shows the mixture temperature (x-axis), absolute humidity (y axis), and the relative humidity (isolines identified by legend). The initial ambient absolute humidity (1) and the space between the "Target-Low" (blue dashed line) and "Target-High" (red dashed line) represent the upper and lower water addition limits. The slope line is the evaporative cooling line, where-in as water is added to increase both the absolute and relative humidity, the mixture temperature falls along this slope. The cathode inlet target Temperature & RH are shown with the green box.

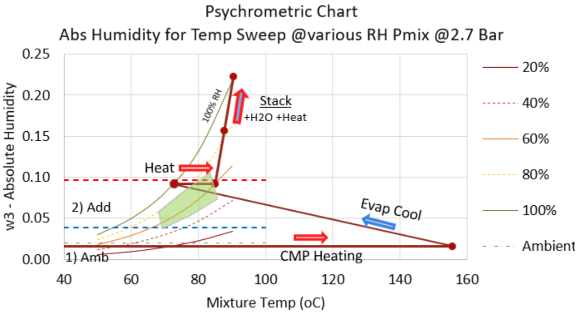

Figure 28. Water-Temperature Trajectory

While this configuration requires a water injector and a heat exchanger, it has eliminated the original "oversized" heat-exchanger which cools the air to the safe cross-flow membrane allowable temperature before water addition. The resulting cooler air is "less hungry" for water, so adding moisture at this stage is a challenge. Thus, the DWI configuration can reduce the size, weight and flow restriction of the heat exchanger and cross-flow membrane, by first adding water and getting evaporative cooling and then run it through a "polishing" heat exchanger, which can be smaller, lighter, and less flow resistive. These trajectories are seen in the figure. Once the evaporative cooling is such that the point reaches the 100% RH / dew-point line, it is a simple matter of increasing the temperature to "glide" into the target box. Also, if more water is required, it can be injected as additional water with droplets which would vaporize in the heat exchanger or a second injector after the heat exchanger. In the end the cathode inlet T and RH conditions are met. Following these, it is evident that water is added in the stack and there is additional heating in the stack as well. The outcome is 100% RH conditions at the temperature leaving the cathode and stack.

6 SUMMARY

This paper has covered multiple concepts related to fuel cell systems and the impact of BoP components on the overall system behavior. In particular, the challenge of maintaining optimum humidity levels in the fuel cells while cooling the hot air supplied by the compressor was highlighted, starting from an outline of the relevant thermodynamics associated with air and water mixtures. A detailed description of the Water-Temperature-Trajectory Approach was used to solve the cathode humidity problem for one particular embodiment. It has demonstrated that while the cathode-air humidity problem is multi-dimensional, it is tractable by using a physics-based modelling approach and the Psychrometric Chart as the "design space" graphic. With this comprehensive approach, we aim to enhance the power, efficiency, reliability, and durability of fuel cell systems. Based on simulation and experiments at our test rig we have also suggested an illustrative example which can be added to or replace a conventional cross-flow membrane-based humidifier for aerospace and industrials applications.

7 CONCLUSIONS

This analysis has laid out a path to design a cathode air stream which meets the cathode inlet and outlet requirements in such a way as to reduce the size, weight, pressure drop and complexity of the system; to demonstrate the path with 0-D thermodynamic, 1-D, and 3-D modeling and simulations, followed by hardware build and test in a fully capable "true-size" test rig. While this is still work in progress, it is clear that with proper trajectory planning, we can use the evaporative cooling effect to improve the overall system design and improve control over pre-cooled, cross-flow, membrane-base humidifier. Ongoing development efforts will focus on scaling these solutions for larger applications and integrating advanced technologies to meet demands of clean energy markets.

8 ACKNOWLEDGEMENTS

The authors would like to thank Manuel Rudolph and Philipp Ruez at EKPO for their assistance. Nolan Polley for CFD simulations. The leadership at Woodward for supporting this project.

9 DEFINITION OF TERMS

AH	Absolute Humidity
AUX	Auxiliary
BoP	Balance of Plant
CFD	Computational Fluid Dynamics
DOE	Design of Experiments
DWI	Direct Water Injection
EGR	Exhaust Gas Recirculation
EID	Electronic Interface Device
0D	Zero-Dimensional
1D	One-Dimensional
3D	Three-Dimensional
FC	Fuel Cell
H2	Hydrogen
H2O	Water
ICE	Internal Combustion Engine
LH2	Liquid Hydrogen
LHV	Lower Heating Value
LWIU	Liquid Water Injection Unit
N2	Nitrogen
O2	Oxygen
PDA	Phase Doppler Anemometry
PEM	Polymer Electrolyte Membrane
PR	Pressure Ratio
RFD	Requirements Flow-Down Model
RH	Relative Humidity

10 APPENDIX

Humidity Equations

$$RH = \phi = \frac{P_v}{P_g}$$

$$AH = \omega = \frac{M_v}{M_a} = 0.622\,\frac{\phi\, P_g}{\left(P_{mix} - \phi\, P_g\right)}$$

$$\dot{M}_w = \omega \dot{M}_a$$

$$P_g = P_{sat}(T) = a_3 T^3 + a_2 T^2 + a_1 T^1 + a_0$$

$$\dot{M}_{H2O} = 1\,\frac{\hat{M}_{H2O}}{\hat{M}_{H2}}\dot{M}_{H2}$$

$$P_v = \frac{\omega}{(0.622 + \omega)} P_{mix}$$

$$\phi = \frac{\omega}{(0.622 + \omega)} \frac{P_{mix}}{P_g}$$

$$T_3 = \frac{(Cp_a - \omega_1 Cp_v)\, T_1 + (\omega_3 - \omega_1)\left(h_v^o - h_f^o\right) + (\omega_3 - \omega_1)\, T_2}{(Cp_a - \omega_3 Cp_v)}$$

$$T_{dp} = T_{sat}(P_w) = \left(b_1 Ln(P_w) + b_o\right)^{-1}$$

$$T_{cmp} = \left(\frac{1}{\eta_{cmp}}\left[PR^{(\gamma-1)/\gamma} - 1\right] + 1\right) T_o$$

11 REFERENCES AND BIBLIOGRAPHY

[1] O'Hayre, Ryan P. *Fuel Cell Fundamentals*. Third ed., J. Wiley & Sons, 2009.

[2] Pukrushpan, Jay T., et al. "Control-Oriented Modeling and Analysis for Automotive Fuel Cell Systems." *Journal of Dynamic Systems, Measurement, and Control*, vol. 126, no. 1, 2004,

https://doi.org/10.1115/1.1648308.

[3] Reynolds, W.C. and Perkins, H.C; "Engineering Thermodynamics, Second Edition", McGraw-Hill, 1977

[4] Pukrushpan, Jay T. *Modeling and Control of Fuel Cell Systems and Fuel Processors*. 2003. University of Michigan, Doctor of Philosophy in Mechanical Engineering.